

Monooxomolybdenum(VI) Complexes Possessing Olefinic Dithiolene Ligands: Probing Mo–S Covalency Contributions to Electron Transfer in Dimethyl Sulfoxide Reductase Family Molybdoenzymes

Hideki Sugimoto,^{*,†} Susumu Tatemoto,[†] Koichiro Suyama,[‡] Hiroyuki Miyake,[‡] Regina P. Mtei,[§] Shinobu Itoh,^{*,†} and Martin L. Kirk^{*,§}

[†]Department of Material and Life Science, Graduate School of Engineering, Osaka University, 2-1 Yamadaoka, Suita, Osaka 565-0871, Japan, [‡]Department of Chemistry, Graduate School of Science, Osaka City University, 3-3-138 Sumiyoshi-ku, Osaka 565-8585, Japan, and [§]Department of Chemistry and Chemical Biology, The University of New Mexico, MSC03 2060, 1 University of New Mexico, Albuquerque, New Mexico 87131-0001

Received April 27, 2010

A monooxomolybdenum(VI) model complex for the oxidized active site in the DMSOR family of molybdoenzymes has been synthesized and structurally characterized. The compound was obtained from the desoxomolybdenum(IV) derivative by clean oxygen-atom transfer from an amine *N*-oxide in a manner similar to that observed in the enzyme. A combination of electronic absorption and resonance Raman spectroscopies, coupled with the results of bonding and excited-state calculations, has been used to provide strong support for a highly covalent Mo(*d*_{xy})–S(dithiolene) π^* -bonding interaction in the molybdenum(VI) complex. It is proposed that the resulting Mo–S covalency facilitates electron-transfer regeneration of the catalytically competent DMSOR Mo^{IV} active site.

The dimethyl sulfoxide reductases (DMSORs) and trimethylamine *N*-oxide reductase (TMAOR) are pyranopterin-containing molybdenum enzymes that catalyze the reduction of Me₂SO and Me₃NO to Me₂S and Me₃N, respectively, and serve as terminal electron acceptors during anaerobic growth of bacteria.^{1,2} In the oxidative half-reaction, a five-coordinate desoxomolybdenum(IV) center abstracts an oxygen atom from the substrate, yielding the reduced product and a six-coordinate Mo^{VI} center that is coordinated by a terminal oxo, a serinate oxygen, and the olefinic dithiolene chelates of two pyranopterin cofactors (Figure 1).³ The absorption spectrum of the oxidized Mo^{VI} site in DMSOR (DMSOR_{ox}) is dominated by low-energy ligand-to-metal charge-transfer (LMCT) transitions at $\sim 14\,000$ and $\sim 18\,300\text{ cm}^{-1}$ that arise from covalent interactions between

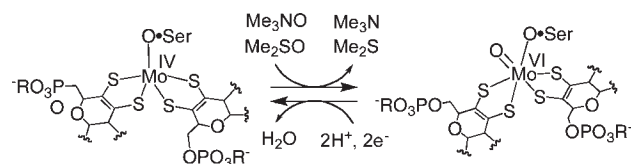


Figure 1. Representation of the catalytically active desoxomolybdenum(IV) and monooxomolybdenum(VI) structures in DMSOR and TMAOR.

the Mo^{VI} center and the dithiolene donors.⁴ The resonance Raman (rR) spectrum of DMSOR_{ox} reveals two dithiolene $\nu(\text{C}=\text{C})$ stretches at 1578 and 1527 cm^{-1} , and this is consistent with crystallographic results that show the two dithiolene chelates to be inequivalent.⁵ The bis(dithiolene) coordination in DMSOR family enzymes has been suggested to modulate the redox potential of the active site, facilitate electron transfer (ET) regeneration of the Mo^{IV} center, and activate the active site for oxygen-atom transfer via the entatic principle.^{6–8} As such, monooxomolybdenum(VI) model compounds that possess bis(dithiolene) ligation and a six-coordinate distorted octahedral coordination geometry provide much needed benchmarks for understanding the relationship between the catalytic mechanism and active-site geometric and electronic structures.^{9,10}

Square-pyramidal desoxomolybdenum(IV) complexes coordinated by olefinic dithiolene ligands have been prepared by Holm et al. and serve as symmetrized structural and functional analogues for the Mo^{IV} center found in reduced DMSOR

*To whom correspondence should be addressed. E-mail: sugimoto@mls.eng.osaka-u.ac.jp (H.S.), shinobu@mls.eng.osaka-u.ac.jp (S.I.), mkirk@unm.edu (M.L.K.).

(1) Hille, R. *Chem. Rev.* **1996**, *96*, 2757.
(2) Burgmayer, S. J. N. *Prog. Inorg. Chem.* **2004**, *52*, 491.
(3) Li, H.-K.; Temple, C.; Rajagopalan, K. V.; Schindelin, H. *J. Am. Chem. Soc.* **2000**, *122*, 7673.
(4) Cobb, N.; Conrads, T.; Hille, R. *J. Biol. Chem.* **2005**, *280*, 11007.

(5) Garton, S. D.; Hilton, J.; Oku, H.; Crouse, B. R.; Rajagopalan, K. V.; Johnson, M. K. *J. Am. Chem. Soc.* **1997**, *119*, 12906.
(6) Kirk, M. L.; Helton, M. E.; McNaughton, R. L. *Prog. Inorg. Chem.* **2004**, *52*, 111.
(7) McNaughton, R. L.; Lim, B. S.; Knottenbelt, S. Z.; Holm, R. H.; Kirk, M. L. *J. Am. Chem. Soc.* **2008**, *130*, 4628.
(8) Webster, C. E.; Hall, M. B. *J. Am. Chem. Soc.* **2001**, *123*, 5820.
(9) Enemark, J. H.; Cooney, J. J. A.; Wang, J.-J.; Holm, R. H. *Chem. Rev.* **2004**, *104*, 1175.
(10) Sugimoto, H.; Tsukube, H. *Chem. Soc. Rev.* **2008**, *37*, 2609.

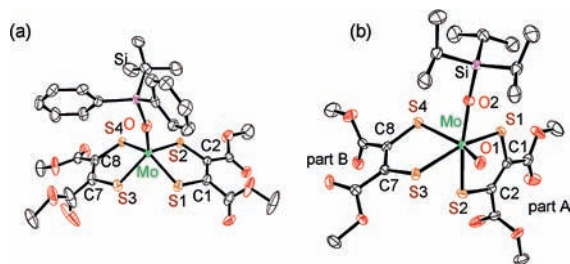


Figure 2. Crystal structures of complexes **1**^{OSiBuPh₂} (a) and **2**^{OSiPr₃} (b) with 50% thermal ellipsoids. Selected bond lengths (Å) and angles (deg): for **1**^{OSiBuPh₂}, S1–C1 1.757(2), S2–C2 1.762(2), S3–C7 1.756(2), S4–C8 1.755(2), C1–C2 1.330(3), C7–C8 1.341(3); for **2**^{OSiPr₃}, Mo–S1 2.4162(9), Mo–S2 2.4778(7), Mo–S3 2.3979(8), S1–C1 1.753(3), S2–C2 1.728(3), S3–C7 1.727(3), S4–C8 1.704(3), C1–C2 1.357(4), C7–C8 1.369(4), O1–Mo–S4 156.90(8), O2–Mo–S2 157.89(8).

(DMSOR_{red}) and other members of the DMSOR enzyme family.¹¹ However, the monooxomolybdenum(VI) species that arise from oxygen atom transfer reactions were too unstable for isolation and full characterization.¹¹ A monooxomolybdenum(VI) bis(dithiolene) complex that possesses aromatic dithiolenes has been synthesized, but the corresponding desoxomolybdenum(IV) compound does not promote clean oxygen atom transfer reaction.^{12,13} We have now synthesized new [Mo^{VI}O(OSiR₃)(dithiolene)₂][−] complexes, which possess biologically relevant olefinic dithiolenes, from their desoxomolybdenum(IV) derivatives by a clean oxygen-atom-transfer reaction. The molybdenum(VI) complexes are six-coordinate and represent excellent structural and reactivity mimics of DMSOR_{ox}. The ability to compare enzyme and model spectroscopic data provides insight into the oxidized DMSOR family active site electronic structure and covalency contributions to ET.

The desoxomolybdenum(IV) complexes [Mo(OSiR₃)(S₂C₂(COOMe)₂)₂][−] [**1**^{OSiR₃} where R₃ = ^{*i*}Pr₃ (**1**^{OSiPr₃}), ^{*i*}BuPh₂ (**1**^{OSiBuPh₂}), S₂C₂(COOMe)₂ = 1,2-dicarbomethoxyethylene-1,2-dithiolate; Chart S1 in the Supporting Information, SI] were prepared from (Et₄N)₂[Mo^{IV}O(S₂C₂(COOMe)₂)₂][−] and the corresponding chlorosilanes. The Mo^{IV} center of **1**^{OSiBuPh₂} exhibits a square-pyramidal geometry, with the OSi^{*i*}BuPh₂ group coordinated axially (Figure 2a). The C=C [1.339(3) and 1.332(3) Å] and C–S [mean 1.758(2) Å] bond lengths support an ene-1,2-dithiolate ligand structure, as is found in all square-pyramidal [Mo^{IV}(OR)(S₂C₂R₂)₂][−] (R = H, Me, Ph) complexes.^{11,12,15,16}

Compounds **1**^{OSiR₃} reacted smoothly with Me₃NO to give a deep-purple solution, although the corresponding reaction with Me₂SO was too slow to be followed. IR spectra of the reaction mixture with Me₃NO display a new band at 880 cm^{−1} assigned as the ν(Mo≡O) stretch (Figure S1 in the SI). Figure 3 shows the time-dependent spectral change of

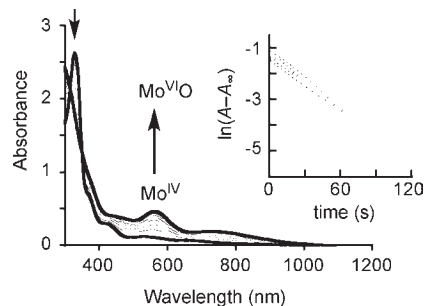


Figure 3. Spectral change for oxygen-atom transfer from Me₃NO (7.5 mM) to **1**^{OSiBuPh₂} (0.15 mM) in CH₃CN at 253 K. (Inset) First-order plot based on the decrease of absorption at 563 nm.

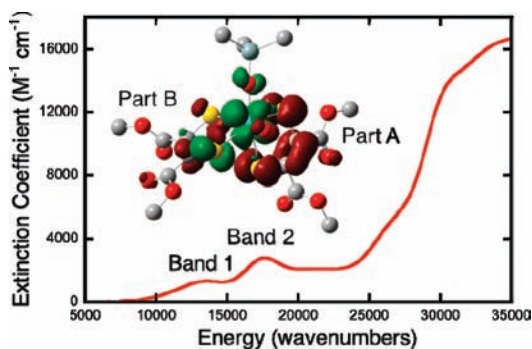


Figure 4. Solution electronic absorption spectrum of **2**^{OSiPr₃}. Inset: Electron density difference map for the transition responsible for band 1. Red indicates a loss of the electron density in the transition, and green indicates a gain in the electron density.

1^{OSiBuPh₂} when treated with Me₃NO. Clear isosbestic points are observed at 351 and 316 nm, indicating that **1**^{OSiR₃} exhibits clean oxygen-atom transfer. The oxygen atom transfer reaction was analyzed kinetically to give parameters of $k^{258} = 5.68 \text{ M}^{-1} \text{ s}^{-1}$, $\Delta H^\ddagger = 8.5 \text{ (kcal mol}^{-1}\text{)}$, and $\Delta S^\ddagger = -15 \text{ (eu)}$ (see Figures S2 and S3 in the SI). The purple species generated from **1**^{OSiR₃} and Me₃NO were stable enough for isolation yielding, [Mo^{VI}O(OSiR₃)(S₂C₂(COOMe)₂)₂][−] (**2**^{OSiR₃}), and the crystal structure of **2**^{OSiPr₃} is depicted in Figure 2b. Compound **2**^{OSiPr₃} possesses a distorted octahedral structure with a S1–S2–S3–S4 dihedral angle of 108°. The terminal oxo exerts a strong trans influence on the Mo–S4 bond, resulting in a long Mo–S4 bond distance [2.5607(8) Å] when compared to the three cis Mo–S bonds [mean 2.431(1) Å], and this underscores a key difference between the two dithiolenes present in **2**^{OSiPr₃}.

The solution electronic absorption spectrum of **2**^{OSiPr₃} (Figure 4) is remarkably similar to that of DMSOR_{ox}, displaying two low-energy bands at 13 533 cm^{−1} ($\epsilon = 1350 \text{ M}^{-1} \text{ cm}^{-1}$) and 17 549 cm^{−1} ($\epsilon = 2800 \text{ M}^{-1} \text{ cm}^{-1}$).⁴ The rR data for **2**^{OSiPr₃} show two dithiolene C=C stretches at 1554 and 1489 cm^{−1}, which are also in good agreement with the enzyme data (Figure 5b) *vide supra*. The latter value is close to those observed in its dioxomolybdenum(VI) analogue, (Et₄N)₂[MoO₂(S₂C₂(COOMe)₂)₂]^{2−} (1494 and 1510 cm^{−1}).¹⁷ Further, vibrational frequency calculations performed on a model for **2**^{OSiPr₃} show C=C stretching modes at 1577 and 1505 cm^{−1} that derive from dithiolenes A and B, respectively (see Figure 2). Only a single C=C stretch is observed at

(11) (a) Lim, B. S.; Holm, R. H. *J. Am. Chem. Soc.* **2001**, *123*, 1920. (b) Wang, J.-J.; Kryatova, O. P.; Rybak-Akimova, E. V.; Holm, R. H. *Inorg. Chem.* **2004**, *43*, 8092. (c) Wang, J.-J.; Tessier, C.; Holm, R. H. *Inorg. Chem.* **2006**, *45*, 2979.

(12) Donahue, J. P.; Goldsmith, C. R.; Nadiminti, U.; Holm, R. H. *J. Am. Chem. Soc.* **1998**, *120*, 12869.

(13) The monooxomolybdenum(VI) complex was prepared from the dioxomolybdenum(VI) derivative and corresponding chlorosilane.¹²

(14) Coucouvanis, D.; Hadjikyriacou, A.; Toupadakis, A.; Koo, S. M.; Ileperuma, O.; Dragonjac, M.; Salifoglou, A. *Inorg. Chem.* **1991**, *30*, 754.

(15) Lim, B. S.; Donahue, J. P.; Holm, R. H. *Inorg. Chem.* **2000**, *39*, 263.

(16) Fomitchev, D. V.; Lim, B. S.; Holm, R. H. *Inorg. Chem.* **2001**, *40*, 645.

(17) Sugimoto, H.; Tatemoto, S.; Suyam, K.; Miyake, H.; Itoh, S.; Dong, C.; Yang, J.; Kirk, M. L. *Inorg. Chem.* **2009**, *48*, 10581.

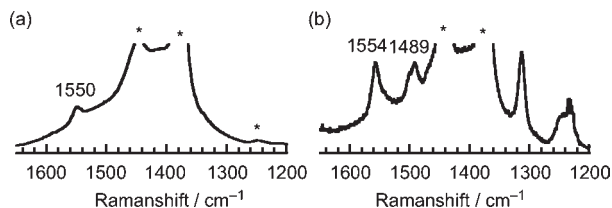


Figure 5. rR spectra of complexes (a) 1^{OSiBuPh_2} (8.6×10^{-3} M) and (b) 2^{OSiPr_3} (2.3×10^{-3} M) in CH_3CN with excitation at 632.8 nm. Asterisks indicate solvent peaks.

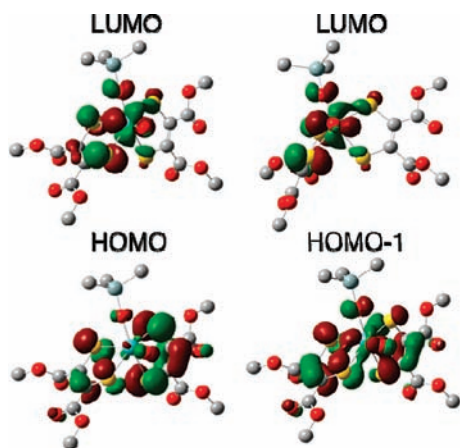


Figure 6. Kohn–Sham orbitals representing relevant molecular orbitals for **2**. The LUMO orientation in the upper right-hand corner is projected down the $\text{Mo}=\text{O}$ bond. In this projection, the LUMO wave function is observed to possess a strong $\text{Mo}(\text{d}_{xy})-\text{S}(\text{p}_z)$ π^* interaction involving the cis $\text{S}(\text{p}_z)$ orbital on dithiolene B.

1550 cm^{-1} for 1^{OSiBuPh_2} (Figure 5a).¹⁸ The rR data underscore the marked inequivalence of the two dithiolenes in 2^{OSiPr_3} with respect to their bonding interactions with the Mo center.

Our bonding and excited-state calculations strongly support an argument whereby the cis $\text{S}(\text{p}_z)$ orbital associated with dithiolene B acts as an acceptor in the low-energy LMCT transitions (Figure 4). Thus, we can assign band 1 as a highest occupied molecular orbital (HOMO) \rightarrow lowest unoccupied molecular orbital (LUMO) transition that displays considerable dithiolene A \rightarrow $\text{Mo}(\text{d}_{xy})$ charge-transfer (CT) character (Figure 4, inset).¹⁹ This derives from the fact that the LUMO is dominantly $\text{Mo}(\text{d}_{xy})$ –dithiolene B in character, while the HOMO possesses nearly equal contributions from both dithiolenes. Band 2 is assigned as a dithiolene A + B \rightarrow $\text{Mo}(\text{d}_{xy})$ CT transition with dominant HOMO–1 \rightarrow LUMO character (Figures 6 and S5 in the SI). Interestingly, the distorted O_h geometry of 2^{OSiPr_3} results

in a LUMO wave function that possesses a strong π^* interaction between the cis $\text{S}(\text{p}_z)$ orbital localized on dithiolene B and the $\text{Mo}(\text{d}_{xy})$ orbital (Figure 6). We previously observed a similar $\text{Mo}-\text{S} \pi^*$ -bonding interaction resulting in a large $\text{Mo}-\text{S}$ covalency and an intense $\text{S}_{\text{thiolate}} \rightarrow \text{Mo}(\text{d}_{xy})$ CT transition in oxomolybdenum thiolate complexes.²⁰ The high $\text{Mo}-\text{S}$ covalency was observed to be a direct result of an $\sim 180^\circ$ $\text{O}_{\text{oxo}}-\text{Mo}-\text{S}-\text{C}$ dihedral angle involving one of the thiolate donors. This geometry properly orients a $\text{S}(\text{p})$ orbital for maximum π overlap with the $\text{Mo}(\text{d}_{xy})$ orbital, resulting in a bonding scheme similar to that observed in blue copper proteins.²¹ A 176° $\text{O}_{\text{oxo}}-\text{Mo}-\text{S}_{\text{dithiolene}}-\text{C}$ dihedral angle involving a single S donor on dithiolene B is present in 2^{OSiPr_3} . This results in the cis S donor of dithiolene B contributing $\sim 18\%$ S character to the LUMO wave function, which is approximately half that found for the blue Cu site ($\sim 35\%$).²¹ The implication here is that the $\text{Mo}(\text{d}_{xy})$ redox orbital in DMSOR_{ox} possesses a strong π -type-bonding interaction with a single $\text{S}_{\text{dithiolene}}$ donor, and this is anticipated to provide a covalent pathway for ET regeneration of the $\text{DMSOR}_{\text{red}}$ site.

In summary, 2^{OSiR^3} are monooxomolybdenum(VI) complexes that coordinate olefinic dithiolene ligands in a manner similar to the Mo active site in DMSOR_{ox} . The complexes can be generated from 1^{OSiR^3} by clean oxygen atom transfer in a manner similar to that observed in the enzymes. A combination of crystallography and electronic absorption and rR spectroscopies strongly supports a unique bonding interaction in 2^{OSiPr_3} and, by inference, DMSOR_{ox} . Low-energy LMCT transitions to a LUMO acceptor orbital that possesses considerable $\text{Mo}(\text{d}_{xy})-\text{S}_{\text{dithiolene}} \pi^*$ character have been assigned. We suggest that the $\text{Mo}(\text{d}_{xy})-\text{S}_{\text{dithiolene}} \pi^*$ -bonding interaction found in 2^{OSiPr_3} may play a key role in facilitating ET regeneration of the $\text{DMSOR}_{\text{red}}$ site. This would occur by coupling the Mo center into hole superexchange pathways that involve a single dithiolene ligand that possesses a S donor ligand cis to the $\text{Mo}=\text{O}$ bond with an $\sim 180^\circ$ $\text{O}_{\text{oxo}}-\text{Mo}-\text{S}_{\text{dithiolene}}-\text{C}$ dihedral angle, as observed in 2^{OSiPr_3} .

Acknowledgment. This work was partially supported by a grant (Grant 22108520 to H.S.) for Scientific Research on Priority Areas “Coordination Programming” from MEXT of Japan. M.L.K. acknowledges the National Institutes of Health (Grant GM-057378) for financial assistance.

Supporting Information Available: X-ray crystallographic data in CIF format, designation of the complexes, experimental details, spectroscopic and crystallographic data, relevant MOs, and an EDDM. This material is available free of charge via the Internet at <http://pubs.acs.org>.

(18) The Fourier transform Raman spectrum of solid 1^{OSiBuPh_2} exhibited one strong peak assigned as the $\nu(\text{C}=\text{C})$ stretch at 1548 cm^{-1} (see Figure S4 in the SI). High moisture sensitivity of 2^{OSiR^3} prevented Raman spectra in the solid state.

(19) *Gaussian 03*, revision C.02; Gaussian, Inc.: Wallingford, CT, 2004.

(20) McNaughton, R. L.; Helton, M. E.; Cosper, M. M.; Enemark, J. H.; Kirk, M. L. *Inorg. Chem.* **2004**, *43*, 1625.

(21) Gewirth, A. A.; Solomon, E. I. *J. Am. Chem. Soc.* **1988**, *110*, 3811–3819.